Petrography, Mineral Composition and Geochemistry of Volcanic and Subvolcanic Rocks of CRP-3, Victoria Land Basin, Antarctica

M. Pompilio[1*], P. Armienti[2] & M. Tamponi[2]

[1]Istituto Nazionale di Geofisica e Vulcanologia, Sezione di Catania - Italy
[2]Dipartimento di Scienze della Terra, Università di Pisa - Italy

**Abstract** - The petrography, mineralogy and geochemistry of volcanic and subvolcanic rocks in CRP-3 core have been examined in detail in order to characterise and to compare them with volcanic and subvolcanic rocks cropping out in the Victoria Land area, and to define the clast provenance or to establish possible volcanic activity coeval with deposition.
Clasts with sizes ranging from granule to boulder show geochemical and mineralogical features comparable with those of Ferrar Supergroup rocks. They display a subalkaline affinity and compositions ranging from basalts to dacite. Three different petrographic groups with distinct textural and grain size features (subophitic, intergranular-intersertal, and glassy-hyalopilitic) are recognised and are related to the emplacement/cooling mechanism.
In the sand to silt fraction, the few glass shards that have been recognised are strongly altered; however chemical analyses show they have subalkalic magmatic affinity. Mineral compositions of the abundant free clinopyroxene grains found in the core, are less affected by alteration processes, and indicate an origin from subalkaline magmas. This excludes the presence, during the deposition of CRP-3 rocks of alkaline volcanic activity comparable with the McMurdo Volcanic Group.
Strong alteration of the magmatic body intruded the Beacon sandstones obliterates the original mineral assemblage. Geochemical investigations confirm that intrusion is part of the Ferrar Large Igneous Province.
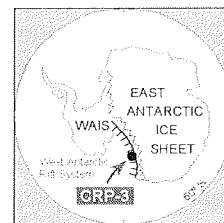
INTRODUCTION

Mackay Glacier drains the East Antarctic ice sheet crossing the Transantarctic Mountains at about 76°. In this sector of the Transantarctic Mountains (TAM) the principal units of the Cambro-Ordovician crystalline basement crop out (Granite Harbour Igneous Complex and Koettlitz Group) (Allibone, 1992; Allibone et al., 1993), as well as the overlying Devonian-Triassic quartzose sedimentary succession (Beacon Supergroup). This sedimentary sequence is intruded and overlain by Jurassic sills and volcanics rocks that form part of the Ferrar Large Igneous Province (FLIP) (Kyle, 1998). The uplift, more than 5 km, of the Transantarctic Mountains began in the late Cretaceous, filling the Ross Sea basins with detrital sediments resulting from denudation (Fitzgerald, 1999). Cenozoic alkalic McMurdo Volcanic Group magmatism began in this sector of the TAM in the Oligocene, as evidenced by volcanic glasses and tephra found in the upper 300 metres cored in CRP-2 (Armienti et al., this volume; McIntosh, 2001) The tephra are the only expression of volcanism in the vicinity of Cape Roberts as surface exposures are lacking. Marine magnetic anomalies, west of the CRP drill sites (Bozzo et al., 1997), may represent the roots of volcanic centres that produced the tephra.

CRP-3 cored about 800 meters of Cenozoic strata, in which igneous materials form an important fraction of the sediments, and about 200 meters of Devonian sandstone intruded by a small magmatic body (Cape Roberts Science Team, 2000).

In this paper we discuss the petrography, mineralogy and geochemistry of volcanic and subvolcanics rocks in CRP-3 in order to characterise and then to compare them with volcanic successions cropping out in the Victoria Land area and finally to define their provenance or to establish possible syndepositional volcanic activity. We investigate as well, compositional and textural characteristics of the magmatic body found at the base of the core, in order to compare it with similar bodies cropping out onland. Further recognition among the volcanic clasts, of distinct lithologies whose stratigraphical positions are well constrained in the onland succession gives information on the uplift and erosion style of the mountain range and on the evolution of the basins.

STRATIGRAPHY OF VOLCANIC AND SUBVOLCANIC ROCKS IN VICTORIA LAND

Volcanic and subvolcanic rocks in Victoria Land were formed in two distinct episodes and contrasting emplacement styles. The older episode, Jurassic in

Corresponding author (pompilio@ct.ingv.it)

age, includes sills (Ferrar Dolerite), lava flows (Kirkpatrick Basalts), and pyroclastic deposits (Mawson and Exposure Hill Formations, Kirkpatrick Basalt pyroclasts) (Elliot, 2000; Elliot et al., 1995). These rocks belong to the Ferrar Supergroup which is now referred to as the Ferrar Large Igneous province (FLIP) (Kyle, 1998). Young volcanics rocks (Eocene to present) formed volcanoes in the McMurdo area and in northern Victoria Land (Kyle, 1990) and are known as the Mc Murdo Volcanic Group (McMVG).

Sills represent the most widespread expression of Jurassic magmatism, in the Transantarctic Mountain, and intrude Beacon Supergroup and rarely the Granite Harbour Intrusive complex. The sills range in thickness from a few tens to over 300 meters (Elliot et al., 1995). They commonly show regular columnar jointing and exhibit sharp intrusive contacts with the host rocks. Rafts of tilted and rotated Beacon strata occur within the sills. Alteration of Beacon sandstones and Ordovician granitoids caused by hydrothermal circulation due to sill intrusion has been documented in the Taylor Glacier region (Craw & Findlay, 1984), and phreatic eruption related to very shallow intrusion has been described as well (Grapes et al., 1973).

Volcanic and volcaniclastic material form the Prebble Formation in the central Transantarctic Mountains, Mawson Formation in South Victoria Land (SVL) and Exposure Hill Formation in northern Victoria Land (NVL) (Elliot, 2000). They overlie a silicic tuffaceous sequence (Hanson Formation) of probable Early Jurassic age (Elliot, 1996) and Triassic volcaniclastic rocks of Lashly, Fremouw and Falla Formations which contain clasts coming from both craton and volcanic arc. In SVL, close to the CRP-3 site, pyroclastic (tuff-breccia and lapilli-breccia of the Mawson formation) and volcaniclastic rocks (Carapace Sandstone) are more than 400 m of thick. Kirkpatrick Basalts form a sequence of lava flows variable from 1 to more than 100 metres thick and with a total thickness in NVL of more than 700 m (Elliot et al., 1986). Lavas are interbedded with volcaniclastic detritus, and locally pillow or pillow-breccia form the base of the lava sequence (Roland & Worner, 1996). Among the Kirkpatrick Basalts two compositional types can be distinguished on the basis of major and trace elements concentrations. The Mt.Fazio chemical type (MFCT) forms the majority the succession, whereas Scarab Peak chemical type (SPCT) forms only the uppermost flows or series of flows. SPCT flows are more evolved than MFCT and shows marked iron and titanium enrichment (Elliot et al., 1995).

Cenozoic magmatic rocks include lavas, tephra (LeMasurier & Thomson, 1990) and intrusions (Tonarini et al., 1997). The extrusive rocks form the youngest stratigraphic unit, except for glacial deposits, in a large part of Victoria Land but intrusion also occur within the Victoria Land basin sediments (Bozzo et al., 1997).

PETROGRAPHY

VOLCANIC AND SUBVOLCANIC CLASTS

Detailed petrographic descriptions of the igneous detritus in CRP-3 are included in the Initial Report (Cape Roberts Science Team, 2000). A summary of the petrographical data is given below. Igneous clasts with sizes ranging from granule to boulder are medium- to fine-grained black to grey rocks. They are generally massive, although amygdaloidal fragments with vesicles filled with secondary minerals are also common.

All the sampled clasts share the same mineral assemblage: major minerals are plagioclase and augite; pigeonite, K-feldspar, orthopyroxene and quartz are also found in most of the samples. Ilmenite and magnetite are ubiquitous accessory minerals. Alteration is significant and mainly affects pyroxenes and the groundmass. Clasts in which the original mineral assemblage is totally replaced by secondary minerals are uncommon. Textural and grain size features observed in thin sections enabled us to divide all the sampled clasts into three groups. These textural differences have been related (Cape Roberts Science Team, 2000) to the cooling rate associated with distinct emplacement mechanisms.

Group I consists of medium to fine-grained holocrystalline rocks, with subophitic texture. Plagioclase is the most abundant phase, forming subhedral crystals (maximum length=2 mm); deuteric sericite alteration commonly replaces crystals. Augite is subordinate and forms subhedral and anhedral crystals (maximum length=4 mm); in most samples it is largely transformed to smectites. Pigeonite is minor as well and is associated with augite as subhedral crystals. Both rhombohedral and cubic Fe-Ti oxides crystals are present in most samples. Less commonly, acicular ilmenite crystals with leucoxene coating are present. In most samples, fine-grained quartz-feldspathic intergrowths are visible in interstices between plagioclase and pyroxene crystals. In fine-grained clasts plagioclase is euhedral, pyroxenes tend to be acicular and a very fine-grained crypto-crystalline matrix is quite often strongly altered to sericite and clay minerals.

Group II is made-up of medium- to fine- grained hypocrystalline rocks with textures varying from intergranular to intersertal. Plagioclase is the most abundant phase and forms a complex network of acicular crystals with pyroxene. Augite crystals are rarely preserved, normally being altered to smectite. Relicts of the original clinopyroxene are preserved only in the cores of few large prismatic crystals. Pigeonite is rare, and orthopyroxene occurs as single prismatic euhedral crystals. Anhedral quartz is present as discontinuous segregations. The interstitial material ranges from very fine-grained cryptocrystalline matrix to very rare palagonitised brown glass that encloses

tiny plagioclase and pyroxene aggregates. Group II clasts are generally non-vesicular, although some irregularly shaped vesicles filled by secondary minerals (carbonate, chalcedony, cristobalite, and zeolites) have been observed.

Group III includes aphyric and weakly porphyritic clasts, generally hypocrystalline but rarely holohyaline. These rocks show a low vesicularity, although in some specimens amygdales filled with secondary minerals form as much as 30% of the rock. Phenocrysts assemblage include hypidiomorphic plagioclase and augite. More than 90% of the rock comprises a quench matrix consisting of acicular crystals of plagioclase and feathery microlites of clinopyroxene and rarely, brown palagonitic glass. In the more vesiculated, scoriaceous clasts, portions with clear brown glass without microlites become predominant.

GLASS SHARDS

The CRP3 Initial Report (Cape Roberts Science Team, 2000) recorded the presence of glass shards in the sand to silt fractions of the CRP-3 core. Thin sections from selected core intervals, where glass shards appeared to be more abundant, have been investigated by optical and scanning electron microscopy (SEM). Glass shards in thin section are difficult to identify due to the very small size (<200 micron) and the flake-like shape. Backscattered SEM images show that they are very finely crystallised (Fig. 1a) and indicate they are not real glass shards as occur in volcanic ash, but rather altered fragments of a glassy or hyalopilitic rocks (Fig. 1 b & c).

INTRUSIVE BODY

Petrographical features of the intrusive body, its variability with depth and the relationship to the host-rocks have been described in detail in the preliminary report. A synthesis is reported here. The rock forming the intrusion is mainly massive and is strongly altered. It is a hypocrystalline, aphyric rock, with a few (<5%) large (2-mm) phenocrysts whose outlines alone are only recognizable. Phenocrysts are tabular sericitised plagioclase and prismatic (augite ?) to equant (ortho ?) pyroxenes totally replaced by hematite, chlorite, clay minerals and carbonate. Samples from the upper part (at 902.13, 903.30 metres below sea floor (mbsf)) tend to preserve the original texture better, although the original mineralogy can be detected only with the scanning electron microscope (Fig. 1d).

The groundmass has a texture varying from intersertal to intergranular and is composed mainly of altered subhedral plagioclase (now sericite). Between the plagioclase laths, reddish hematite grains are abundant and probably are replaced mafic minerals. Interstitial areas with acicular feldspars (albite or K-

feldspar), smectites, serpentine and ilmenite needles are also found and have probably replaced original glass (Fig. 1d).

In samples from the lower portion of the intrusion (depth >906 mbsf), the texture, as well as the original mineralogy, is totally destroyed: an anastomising web of carbonates, smectites, probable serpentine, and hematite has completely replaced most of the rock (Fig. 1e).

MINERAL CHEMISTRY

Chemical analyses of phases were carried out with both wavelength dispersive (Cameca-Camebax microprobe at CNR-CSESMR Rome at 20 kv of acceleration tension, 30 mA of probe current, spot size variable from 5 μm in minerals to 20 μm in glasses) and energy dispersive systems (SEM Cambridge S360 and Link Exl EDS microanalysis at INGV-Catania with 15 kv, 0.5 mA, spot size 5–20 μm) using natural minerals as standards and ZAF corrections.

The composition of minerals (phenocrysts or microlites) found in volcanic clasts and as crystal fragments are reported in tables 1 and 2 and in figure 2.

Plagioclase composition range from An_{80} to An_{40}; more anorthitic compositions are found in phenocrysts belonging to Group I clasts (An_{80-52}) (Tab. 1 and Fig. 2a). The highest anorthite contents are found in phenocryst cores and rims and microphenocrysts are systematically more albitic. A larger compositional range in plagioclase is reported for basal dolerite boulder in CIROS-1 (Grapes et al., 1989) and in volcanic detritus of CRP-1 and 2 (Armienti et al., 1998; Armienti et al. this volume). In particular in CRP-1 and 2 cores an abundance of anorthose crystals attributable to McMurdo Cenozoic magmatism was observed (Armienti et al., 1998). Conversely the compositional range observed in feldspars of CRP-3 volcanic detritus, lies whitin that measured in Ferrar dolerites and Kirkpatrick basalts (both MFCT and SPCT types) reported in Elliot et al. (1995) and Hornig (1993) (Fig. 2a). Most of the analysed pyroxenes are augites with a distinct iron-enrichment trend (Tab. 2 & Fig. 2b). A small subset of data exhibits subcalcic augite and pigeonite composition which is also observed petrographically. This compositional range is typical of subalkaline volcanic rocks of the Ferrar Supergroup (Elliot et al., 1995; Hornig, 1993). In the Ca+Na vs Ti discriminant diagram (Leterrier et al., 1982) (Fig. 3), CRP-3 clinopyroxenes fall in the subalkali field together with subalkaline pyroxenes that characterise diamictite of the lower portion of CRP-2. Sodic pyroxenes observed among the clasts and crystal fragments in CRP-1 and 2 (Armienti et al., 1998) are totally lacking in CRP-3 suggesting that the whole
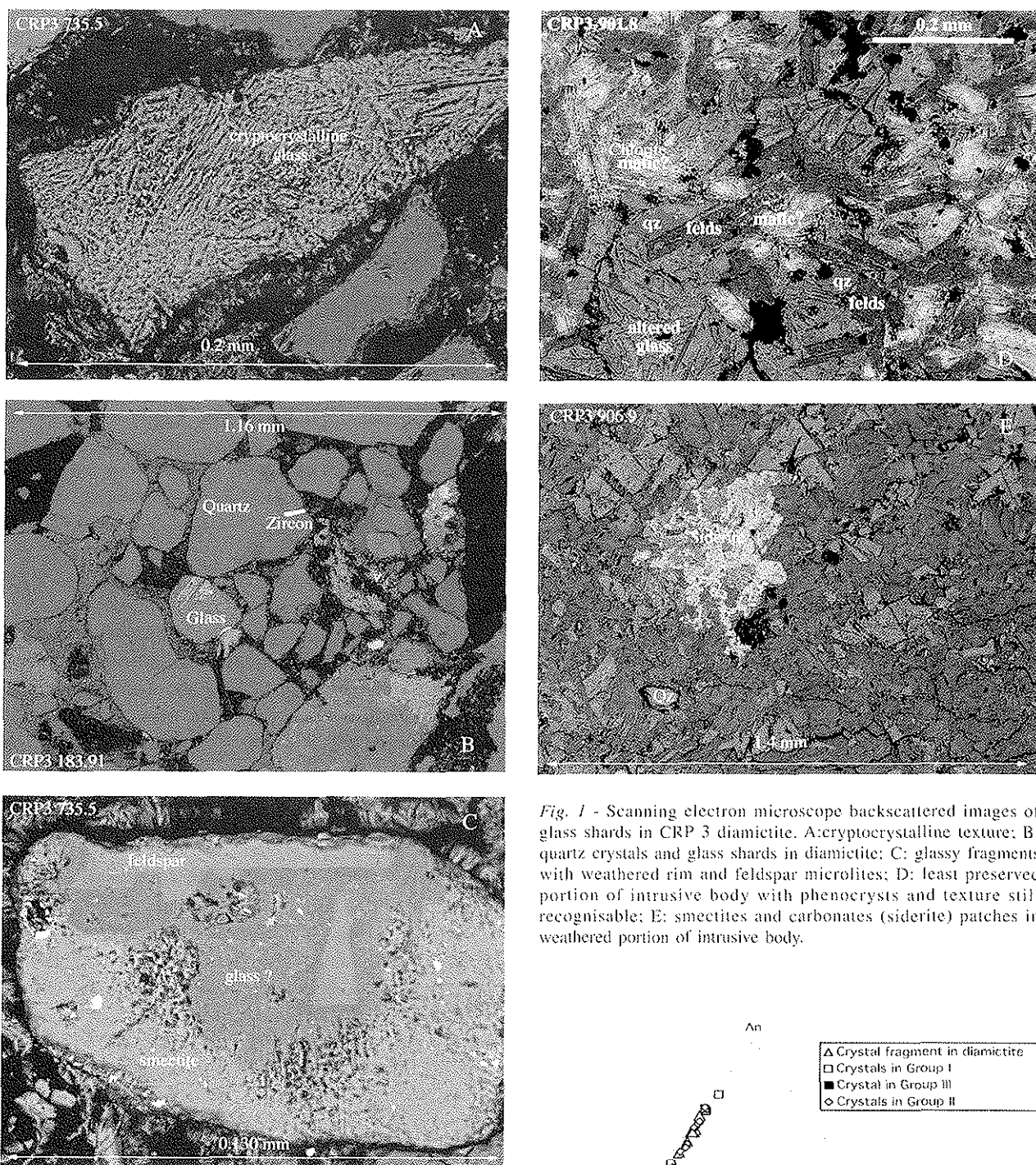
Fig. 1 - Scanning electron microscope backscattered images of glass shards in CRP 3 diamictite. A:cryptocrystalline texture; B: quartz crystals and glass shards in diamictite; C: glassy fragments with weathered rim and feldspar microlites; D: least preserved portion of intrusive body with phenocrysts and texture still recognisable; E: smectites and carbonates (siderite) patches in weathered portion of intrusive body.

Fig. 2 - Compositions of plagioclases (A) and pyroxenes (B) occuring in clasts or as crystal fragments in CRP-3 core.

sedimentary pile was deposited before onset of the Cenozoic McMVG magmatism in the area.

In the intrusive body drilled at the bottom of CRP-3 (901.09-919.95 mbsf), the original magmatic paragenesis is totally replaced by deuteric minerals. Some pseudomorphs with the original shapes of pyroxenes and feldspars are present but the original composition has been completely erased. Widespread patches of siderite characterise the groundmass of the intrusive body (Fig. 1e), showing that fluids played an important role in the alteration of the intrusion.
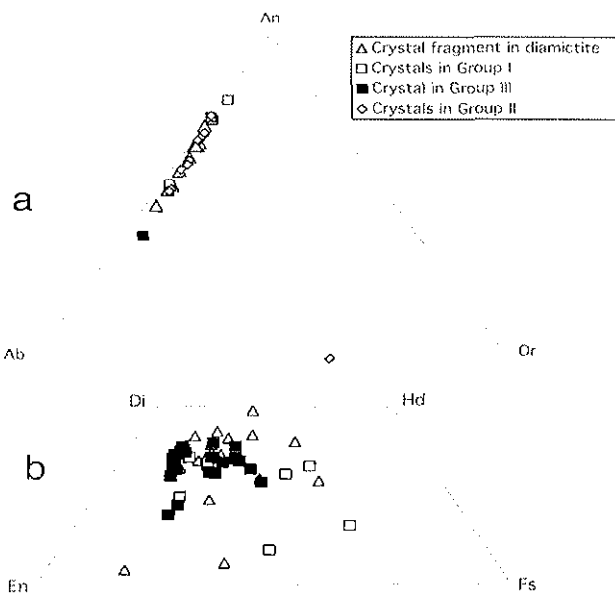
Tab. 1 - Compositions of selected plagioclase crystals in CRP-3 core.

Depth (mbsf)	5.93	5.93	5.93	183.91	183.91	183.91	163.3	185.5	370.8
Group/Type	I-f	I-f	I-f	II-f	II-f	II-f	III-f	free	free
SiO₂	53.90	49.44	47.88	51.83	55.27	51.80	57.52	54.25	51.61
Al₂O₃	27.26	30.63	31.49	28.77	27.66	29.07	25.35	27.93	28.84
FeO	0.80	0.87	0.74	0.63	1.30	0.59	0.40	0.41	0.86
MgO	0.00	0.00	0.00	0.00	0.00	0.32	0.31	0.00	0.29
CaO	10.98	14.59	15.93	13.73	11.84	13.78	7.60	10.95	13.13
Na₂O	5.04	2.80	2.18	3.43	4.51	3.25	6.44	5.03	3.69
K₂O	0.29	0.00	0.15	0.21	0.35	0.17	0.65	0.47	0.27
Tot.	98.27	98.33	98.37	98.6	100.93	98.98	98.27	99.04	98.69

Formula recalculated on the basis of 8 oxygen

Si	2.480	2.293	2.231	2.390	2.479	2.378	2.620	2.476	2.379
Al	1.479	1.675	1.730	1.564	1.463	1.573	1.361	1.503	1.567
Fe3+	0.031	0.034	0.029	0.024	0.049	0.023	0.015	0.016	0.033
Mg	0.000	0.000	0.000	0.000	0.000	0.003	0.003	0.000	0.003
Ca	0.541	0.725	0.796	0.678	0.569	0.678	0.371	0.535	0.649
Na	0.450	0.252	0.197	0.307	0.392	0.289	0.569	0.445	0.330
K	0.017	0.000	0.009	0.012	0.020	0.010	0.038	0.027	0.016
An	53.7	74.2	79.4	68.0	58.0	69.4	37.9	53.1	65.2
Ab	44.6	25.8	19.7	30.7	40.0	29.6	58.2	44.2	33.2
Or	1.7	0.0	0.9	1.2	2.0	1.0	3.9	2.7	1.6

GEOCHEMISTRY

VOLCANIC AND SUBVOLCANIC CLASTS AND GLASS SHARDS

Bulk compositions of larger clasts which are representative of the three different petrographical groups are reported in table 3. Microanalyses of glass shards and intergranular glasses in clasts are also included in table 4.

The large loss of ignition (LOI) values measured in the bulk rock samples, the low total for glasses and the occurrence of a small amount of corundum in the CIPW norm, indicate that rocks and shards have been subjected to a significant and variable degrees of alteration.

Chemical alteration was checked using ternary diagrams proposed by Nesbitt & Young (1989) (Fig. 4). In these diagrams, bulk compositions of the largest analysed clasts and mesostasis glasses plot very close to those of basalts-gabbros and show only a limited scatter which is probably related to differentiation processes. In the same diagrams most of the glass shards plot along a differentiation trend whereas only a few glass compositions point toward kaolinite (or kandite) and illite end-members denoting important alteration processes.

On the basis of this diagram, altered glasses were excluded and the less altered compositions plotted in the total alkali-silica (TAS) diagram in order to classify and to compare them with volcanic successions cropping out on land (Fig. 5).

Larger clasts range in composition from basaltic

andesite to dacite. In particular rocks belonging to group I are basalts, whereas group II and group III are respectively, basaltic andesites and dacites. Group I and group II rocks show compositions comparable with those reported by (Elliot et al., 1995) for Ferrar Supergroup rocks. Group III rocks show a more
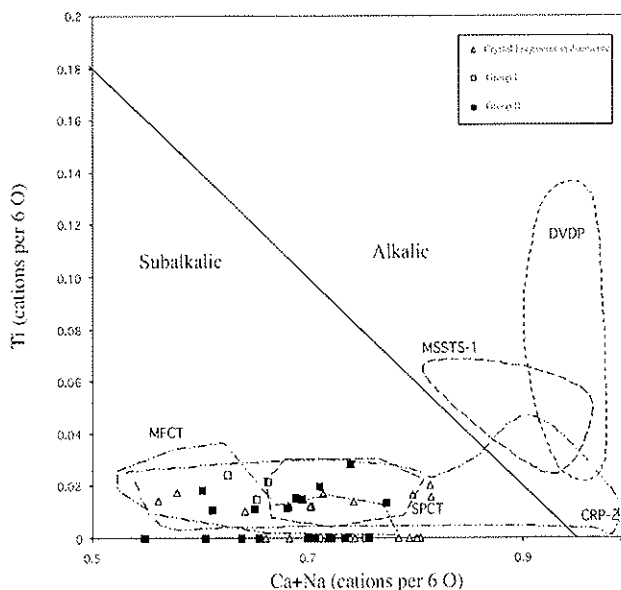
Fig. 3 - Ca+Na vs Ti (cationic units) discrimination diagram (Leterrier et al., 1982) for CRP-3 pyroxenes. Compositional variations observed in pyroxenes belonging to Mount Fazio Chemical Type (MFCT) and Scarab Peak Chemical Type (SPCT) in Ferrar Dolerites and Kirkpatrick Basalts rocks (Elliot et al., 1995; Fleming et al., 1992, 1995; Hornig, 1993) or found in CRP-2 (Armienti et al., 2001), MSSTS-1 (Gamble et al., 1986) and DVDP (Kyle, 1981) cores are reported for comparisons.

Tab. 2 - Compositions of selected pyroxene crystals in CRP-3 core.

Depth (mbsf)	5.93	5.93	5.93	5.93	47.74	727.61	727.61	727.61	5.79	5.79	163.3
Group/Type	I	1	1	I	I	II	II	II	free	free	free
SiO$_2$	49.89	49.80	47.64	51.70	53.30	50.54	50.74	50.77	49.87	53.78	53.08
TiO$_2$	0.83	0.73	0.71	0.00	0.53	0.38	0.53	0.51	0.55	0.38	0.00
Al$_2$O$_3$	1.26	1.03	0.72	1.10	1.89	1.40	1.48	1.54	1.09	1.79	1.61
FeO	22.16	24.10	33.65	27.08	11.89	17.18	15.38	14.92	19.78	8.59	10.20
MnO	0.47	0.43	0.61	0.57	0.39	0.38			0.47		
MgO	10.69	8.55	8.29	16.19	16.61	13.19	13.35	13.62	8.16	18.70	16.64
CaO	15.00	15.72	7.59	4.67	16.53	15.73	16.63	16.84	18.77	16.25	16.97
Tot	100.3	100.36	99.21	101.3	101.14	98.8	98.11	98.2	98.69	99.49	98.5

Formula recalculated on the basis of 4 cations (6 O)

|											
Si	1.939	1.959	1.941	1.965	1.962	1.950	1.962	1.957	1.979	1.980	1.994
Al ^{IV}	0.058	0.041	0.035	0.035	0.038	0.050	0.038	0.043	0.021	0.020	0.006
Fe $^{3+IV}$	0.004	0.000	0.024	0.000	0.000	0.000	0.000	0.000	0.000	0.000	0.000
Al ^{VI}	0.000	0.007	0.000	0.014	0.044	0.013	0.029	0.027	0.030	0.058	0.065
Fe $^{3+ VI}$	0.013	0.000	0.015	0.021	0.000	0.015	0.000	0.000	0.000	0.000	0.000
Ti	0.024	0.022	0.022	0.000	0.015	0.011	0.015	0.015	0.016	0.011	0.000
Mg	0.619	0.502	0.504	0.917	0.912	0.759	0.769	0.783	0.483	1.026	0.932
Fe^{2+}	0.704	0.793	1.107	0.839	0.366	0.540	0.497	0.481	0.656	0.264	0.320
Mn	0.015	0.014	0.021	0.018	0.012	0.012	0.000	0.000	0.016	0.000	0.000
Ca	0.624	0.663	0.331	0.190	0.652	0.650	0.689	0.695	0.798	0.641	0.683
Wo	31.61	33.61	16.75	9.57	33.58	32.91	35.22	35.50	40.86	33.18	35.29
En	31.35	25.44	25.46	46.18	46.95	38.40	39.35	39.95	24.72	53.13	48.15
Fs	37.05	40.95	57.79	44.25	19.48	28.68	25.43	24.55	34.42	13.69	16.56

Formula calculated following IMA rules (Morimoto et al, 1988), Fe^{3+} calculated assuming charge balance.

evolved composition that is rare in the FLIP. With the only exception of one sample described by Brotzu et al., (1988), rocks which are classified as dacites based on geochemistry, are all from evolved regions of sills or interstitial areas in thick lava flows (Elliot et al., 1995).

The glasses are rhyolitic in composition and resemble pyroclastic rocks in the Hanson Formation (redefined Upper Falla formation; Elliot, 1996). Using Zr, Ti, Nb and Y elements, that are considered to be immobile during the weathering and alteration processes, bulk clast compositions are subalkalic and range in composition from basalts to andesite (Fig. 6). In particular, with the exception of a single Group 1 sample, the analysed clasts samples fall outside the fields for MFCT and SPCT rocks described by (Elliot et al., 1995; Roland & Wörner, 1996) and dolerite clasts of CRP-1 (Kyle, 1998). In addition on a Zr vs TiO$_2$ diagrams (Fig. 7) CRP-3 volcanic clasts of group I and one of group II fall along the trend of MFCT and dolerite clasts of CRP-1, whereas group III clasts and one group II clast fall outside.

Fig. 4 - A-CN-K and A-CNK-FM diagrams (molar proportion) for glasses (shards and clast mesostasis), bulk clasts and intrusive body of CRP-3 core. Heavy curve with arrow represents a differentiation trend from gabbro to granite, dashed lines describe weathering trends (Nesbitt & Young, 1989).
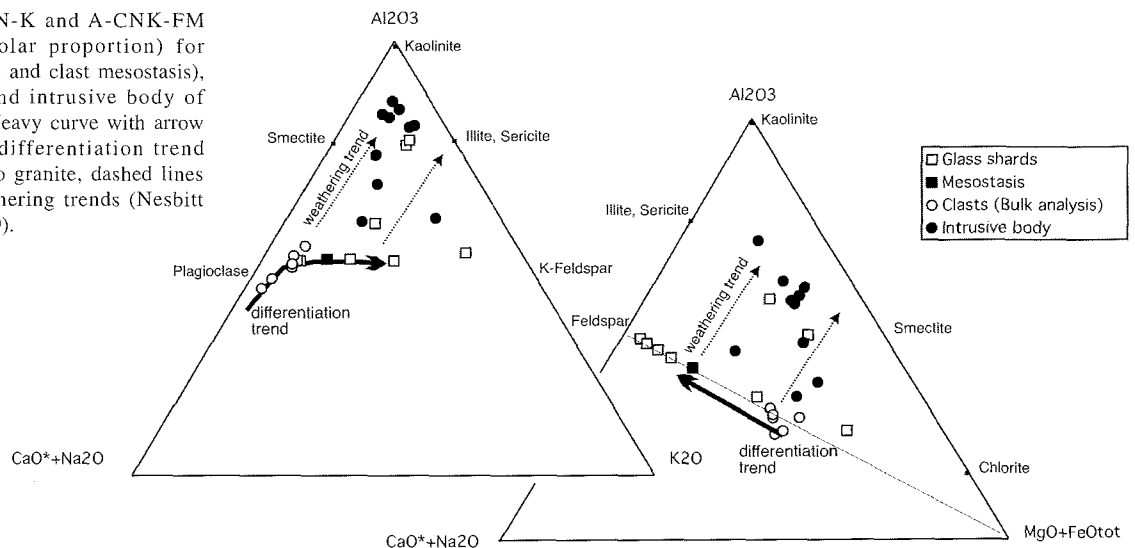
Tab. 3 - Major and trace element bulk-rock composition of selected CRP-3 clasts.

Depth (mbsf)	33.60-66	344.61-64	184.34-39	387.05-08	469.24-28	627.11-14
Petrographic group	I	I	II	II	III	III
SiO_2	56.47	51.22	62.43	59.08	63.60	63.70
TiO_2	0.89	0.95	0.69	1.27	0.83	0.91
Al_2O_3	14.40	16.85	12.70	13.67	12.50	12.78
Fe_2O_3	2.73	7.13	2.77	5.66	3.00	3.55
FeO	7.48	8.01	5.35	5.46	5.22	4.11
MnO	0.16	0.04	0.13	0.11	0.11	0.11
MgO	4.54	1.76	4.64	2.87	3.86	3.40
CaO	8.08	5.85	5.91	4.72	3.31	4.38
Na_2O	1.92	2.47	2.07	2.68	2.17	2.31
K_2O	1.03	1.72	1.01	1.69	1.49	1.51
P_2O_5	0.12	0.12	0.10	0.17	0.11	0.11
LOI	2.18	3.88	2.21	2.62	3.81	3.12
Tot	100.00	100.00	100.01	100.00	100.01	99.99
Mg#	51.71	21.64	58.92	38.93	54.16	53.01
Q norm	15.69	8.26	25.61	19.32	30.45	28.39
C norm		0.60			1.63	
Nb	6	7	7	13	8	10
Zr	144	132	163	224	189	207
Y	31	17	25	37	21	19
Sr	135	131	141	136	125	124
Rb	44	96	50	70	71	69
Ce	39	34	34	59	32	39
Ba	291	253	224	462	307	342
La	19	13	16	23	12	17
Ni	56	37	51	33	43	45
Cr	57	114	100	35	62	61
V	247	303	207	287	230	235
Co	45	40	34	41	34	34

Analyses carried out at DST-Pisa on powder pellets, using a Philips PW1480 XRF spectrometer, with a full matrix correction of Franzini et al. (1975) and Leoni & Saitta (1976), MgO and Na_2O were determined by AAS, FeO by titraton, LOI gravimetrically.

In conclusion, no analysed clast is comparable to SPCT rocks, but taking into account the scatter caused by alteration and/or possible analytical bias most of the analysed clasts can be related to the MFCT rocks.

INTRUSIVE BODY

Eight samples representing the central portion of the igneous intrusion (see table 5 for depth of sampling and analyses) and larger clasts enclosed in the external fractured zones were analysed for major and trace elements by XRF at Victoria University, Wellington and Pisa University. Any systematic difference is detectable between samples analysed from two laboratories, and thus inter-laboratory bias can be considered not-significant.

The chemical compositions of these rocks confirm the occurrence of extensive alteration, as clearly shown in petrographical observations. In all samples,

major element concentrations appear to be strongly modified by alteration processes as suggested by large loss of ignition values (LOI) and normative corundum in the CIPW norm. In the ternary diagrams of Nesbitt & Young (1989) (Fig. 5), samples from the intrusive body plot along weathering lines mainly controlled by the alteration of plagioclase and formation of smectite and in some cases illite. In both diagrams, these intrusive rocks display a wide scatter probably reflecting varying degrees of alteration. In figure 8 LOI and ratios between mobile (Fe, Mg) and immobile (Ti, Nb) elements during alteration are plotted against the depth. Though petrographical observations indicate more pronounced alteration in the lower portion of the igneous body (below 906.00 mbsf) no clear correlation is evident between the above compositional parameters and the depth. On the other hand, peaks with high LOI, FeO_{tot}/TiO_2, MgO/TiO_2 at 909 and 915 mbsf confirm that some portions of the intrusion suffered significant changes
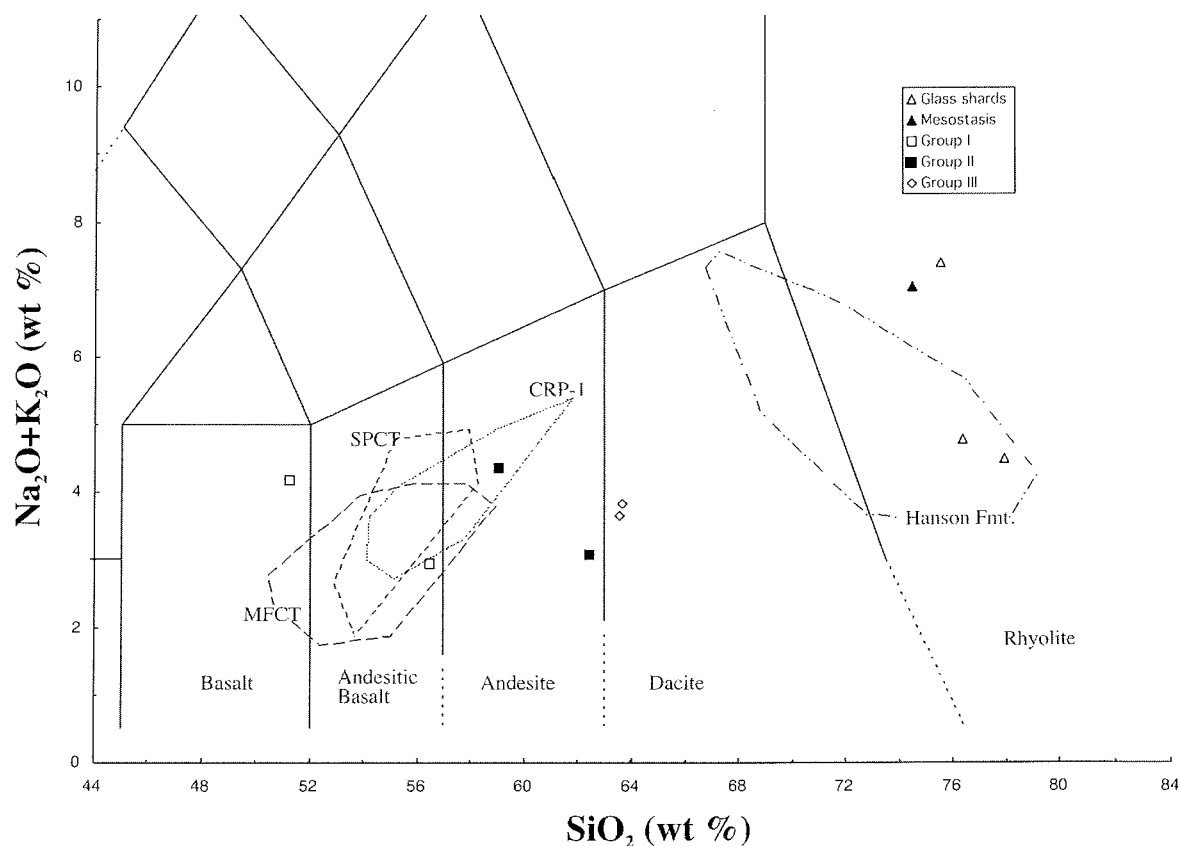
Fig. 5 - Total Alkali -Silica (TAS) classification diagram for selected, less altered volcanic rocks in CRP-3 core. Fields for Mount Fazio Chemical Type (MFCT) and Scarab Peak Chemical Type (SPCT) in Ferrar Dolerite and Kirkpatrick basalt rocks (Elliot et al., 1995; Fleming et al., 1992, 1995; Hornig, 1993), volcanics rocks in CRP-2 (Armienti et al., 2001) and rocks from the Hanson Formation (Elliot & Larsen, 1993) are reported for comparisons.

Tab. 4 - Average composition of glass shards and glassy mesostasis in CRP-3 core.

depth	5.79	47.74	185.5	185.5	370.8	375.3	735.4 group II mesostasis
# ans	2	1	4	2	1	1	2
SiO_2	59.90	56.37	75.60	76.41	77.96	76.01	74.54
TiO_2	1.42	1.02	0.00	0.79	0.00	0.16	0.00
Al_2O_3	25.17	15.21	13.93	12.33	12.34	14.87	13.35
FeOtot	4.36	14.21	0.61	2.49	1.11	2.20	1.84
MnO	0.00	0.00	0.00	0.00	0.00	0.01	0.00
MgO	1.90	4.93	0.07	0.00	0.00	3.17	1.22
CaO	0.31	2.20	2.36	3.14	3.35	0.05	2.01
Na_2O	1.63	1.47	3.05	3.08	2.93	0.98	3.95
K_2O	4.39	4.25	4.34	1.69	1.56	2.54	3.09
P_2O_5	0.00	0.00	0.00	0.00	0.64	0.00	0.00
Cl	0.93	0.35	0.03	0.07	0.12	0.00	0.00
Range of totals in original analyses	72-73	79	79-96	94-97	94	72	94-95
Mg#	50.6	44.0	22.8	0.0	0.0	78.8	63.2
Q norm	29.1	12.2	35.8	44.9	49.1	54.8	32.9
C norm	17.3	4.2	0.0	0.0	1.3	10.4	0.0

Analyses are normalised to 100.

Tab. 5 - Major and trace element of the magmatic intrusive body.

Interval	c	c	c	c	c	c	c	c	d	e
SiO$_2$	50.2	56.53	54	46.37	34.24	46.66	38.52	48.4	49.98	81.75
TiO$_2$	0.92	1.01	0.97	0.74	0.62	1.01	0.64	0.93	0.86	0.18
Al$_2$O$_3$	24.11	24.57	20.97	22.1	15.91	25.18	15.29	24.12	24.86	7.82
Fe$_2$O$_3$	3.91	4.87	8.55	1.47	20.64	8.02	18.46	6.3	3.15	1.08
FeO	3.85			8.45		2.18		4.01	5.11	1.38
MnO	0.05	0.01	0.06	0.09	0.16	0.04	0.18	0.1	0.05	0.02
MgO	1.99	0.92	1.23	1.69	2.19	1.84	2.74	1.14	1.33	0.6
CaO	0.75	0.57	0.8	2.21	2.4	0.59	3.78	0.94	0.72	0.76
Na$_2$O	0.43	0.56	0.63	0.54	0.19	0.51	0.12	0.84	0.5	0.17
K$_2$O	3.57	2.4	1.88	2.67	2.87	3.94	3.6	1.66	1.75	3.44
P$_2$O$_5$	0.02	0.03	0.13	0.07	0.1	0.14	0.11	0.13	0.01	0.08
LOI	10.19	9.36	10.71	13.6	20.91	9.89	17.46	11.44	11.68	2.71
Tot.	99.99	*100.83	*99.93	100	*100.23	100	*100.9	100.01	100	99.99
Mg#	37.94	32.98	27.26	28.13	19.87	29.17	25.76	21.05	27.48	39.73
Q norm	28.99	43.89	41.23	24.13	3.07	21.98	2.18	32.80	37.37	66.18
C norm	20.34	22.05	18.92	16.73	10.79	21.62	5.60	22.17	23.65	2.70
Nb	9	7	8	7	5	9	3.5	9	8	7
Zr	146	163	144	113	95	156	98	140	137	360
Y	26	13	27	31	34	30	50	38	18	32
Sr	58	84	150	60	61	56	56	67	78	69
Rb	202	70	75	143	64	218	181	88	79	147
Ce	43	38	65	33	29	33	30	43	32	73
Ba	361	179	198	343	577	621	521	246	225	513
La	9	15	18	7	21	12	10	17	13	59
Ni	56	36	57	48	51	123	98	47	43	27
Cr	102	75	73	80	150	154	135	77	80	13
V	173	149	155	237	194	351	185	196	178	22
Co	38	nd	nd	52	nd	46	nd	40	33	12
As	nd	1	12	nd	2	nd	0	nd	nd	nd
Cu	nd	77	90	nd	110	nd	93	nd	nd	nd
Ga	nd	22	19	nd	21	nd	21	nd	nd	nd
Pb	nd	9	16	nd	9	nd	8	nd	nd	nd
Sc	nd	47	73	nd	52	nd	53	nd	nd	nd
Th	nd	5	5	nd	2	nd	2	nd	nd	nd
U	nd	2	3	nd	0.5	nd	2	nd	nd	nd
Zn	nd	42	66	nd	584	nd	131	nd	nd	nd

*Analysts: R. Grapes, J.E. Patterson (Victoria Univ. Analytical Facility - Wellington, NZ). Remaining analyses carried out at DST Pisa on powder pellets, using an Philips PW1480 XRF spectrometer, with a full matrix correction of Franzini et al. (1975) and Leoni and Saitta (1976), MgO and Na$_2$O were determined by AAS, FeO by titraton, LOI gravimetrically.

in composition due to extensive precipitation of carbonates (mostly siderite) from circulating fluids.

On the basis of the above observation is concluded that major element concentrations do not represent the original compositions of the igneous body and cannot be used to infer magmatic affinity, nor correspondence with volcanic successions cropping out onland.

Minor and trace elements show an analogous variability that can be ascribed to re-mobilisation due to alteration. However, some elements (Ti, P, Zr, Nb, and Y) that are known to be less affected by alteration processes can still be used for comparisons with exposed igneous rocks and to infer magmatic affinities. In figure 6 the samples of the CRP-3 intrusions are plotted in the classification-discrimination diagram of Floyd & Whinchester (1978) which is based on ratios of immobile elements. Even with a significant scatter exists, the samples fall inside the subalkaline field, astride the divide between basaltic and andesitic compositions. These results rule out the association with the alkaline Cenozoic McMVG and suggest a rather close correspondence with the Jurassic Ferrar Supergroup. Samples of the CRP-3 intrusion have Ti-Zr (Fig. 7) and Zr-Nb ratios (Cape Roberts Science Team, 2000) consistent with a Ferrar origin.
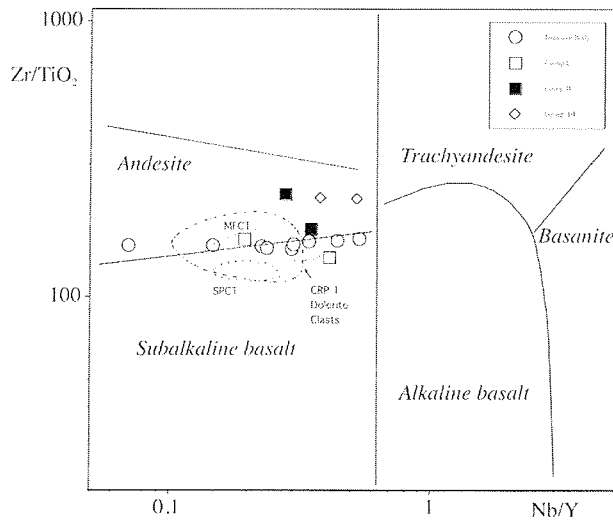
Fig. 6 - Nb/Y and Zr/TiO$_2$ classification diagram (Floyd & Winchester, 1978) for CRP-3 volcanics clasts and intrusive rocks. Fields for rocks belonging to the Mount Fazio Chemical Type (MFCT) and Scarab Peak Chemical Type (SPCT) of the Ferrar Supergroup (Elliot et al., 1995; Fleming et al., 1992, 1995; Hornig, 1993) and dolerite clasts in CRP-1 (Kyle, 1998) are reported for comparison.

CONCLUSIVE REMARKS

Mineral and glass chemistry, bulk clast chemistry and textures of igneous detritus in the CRP-3 confirm they are Ferrar Supergroup material. Even strongly altered clasts show an unequivocal subalkaline affinity typical of Jurassic rocks belonging to the Ferrar Supergroup.

The large textural differences within clasts reflect the cooling rate associated with different emplacement mechanisms. Thus holocrystalline clasts with subophitic textures typical of intrusive magmatic bodies would represent the erosion of Ferrar sills or would belong to the inner portions of thick Kirkpatrick lava flows; intersertal to intergranular textures, with a variable abundance of interstitial glass, could represent the external part of these sills, but more probably they are eroded fragments of Kirkpatrick lava flows. Glass-rich, vesiculated volcanic rocks and quench crystals indicate a high cooling rate, such as that associated with chilling of magma on contact with water or country rocks. Alternatively they may represent the external portions of Kirkpatrick lava flows or alternatively, could be pillow-lava fragments derived from the pyroclastic or volcaniclastic deposits that are intercalated in the Kirkpatrick succession. Bulk chemistry of Group I and Group II clasts roughly matches the compositional range of the MFCT Ferrar Dolerite and Kirkpatrick Basalt. Group III rocks, although subalkaline, show an evolved composition that was not observable in any of the volcanics cropping onland. Finally, rare glass shards show a good correspondence with the Hanson unit, they would therefore derive from the erosion of these volcanics which being probably early Jurassic in age, underlie the Ferrar Supergroup succession. This magmatic affinity excludes these glasses from being products of Cenozoic alkaline activity coeval with their deposition, as hypothesised in the initial report, and indirectly supports the onset of Cenozoic activity in
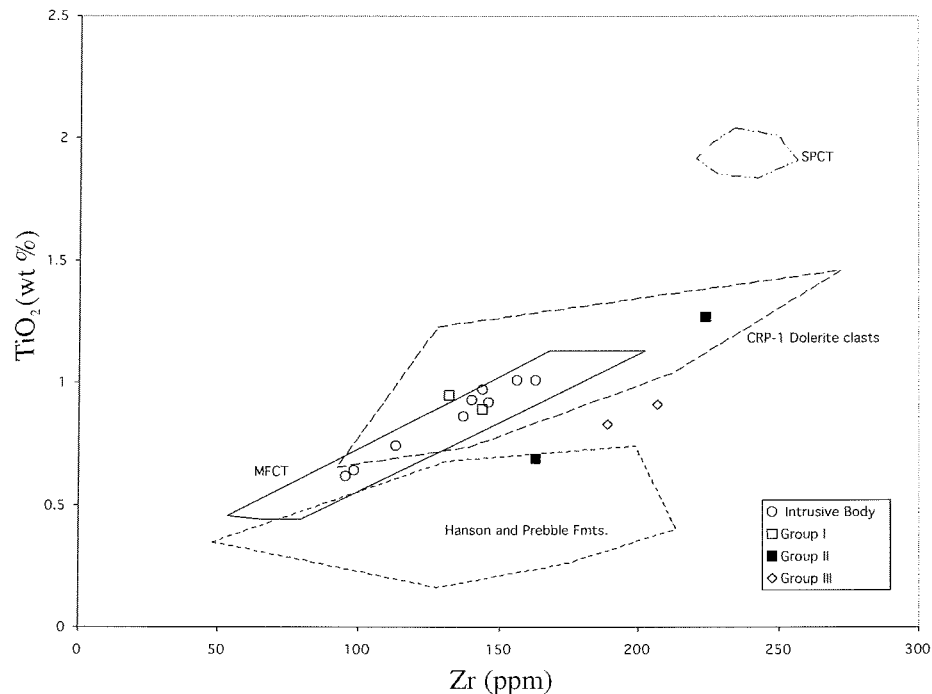

Fig. 7 - Zr vs TiO$_2$ plot for CRP-3 volcanics clasts and intrusive rocks. Data sources for MFCT, SCPT CRP-1 dolerite clasts and Prebble and Hanson Formations are the same as figures 5 and 6.
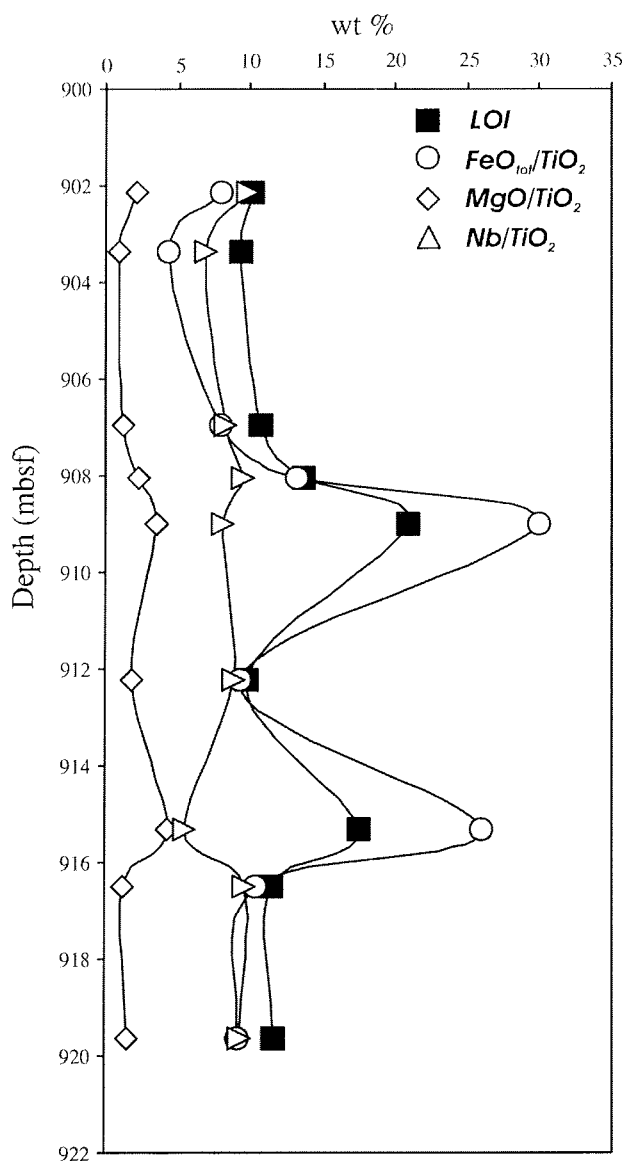
Fig. 8 - Loss of Ignition, FeO-TiO$_2$, Mg-TiO$_2$, Nb-TiO$_2$ ratios *vs* depth for rocks belonging to the intrusive body.

intrusive bodies emplaced into Beacon rocks at various stratigraphic levels. The geometrical relationships between the intrusion and the country rock and the petrographical characteristics of the former can be used to make inferences on the emplacement and cooling styles. The inferred presence of glass points to relatively fast cooling of the margin of the magmatic body, whereas the occurrence of breccia in a clay-rich zone indicates an important episode of brittle deformation and hydrothermal alteration at a lower temperature that accompanied or followed the emplacement. These processes caused modification of the outer part of the intrusion mechanical and chemical. The lack of vesiculation excludes emplacement at very shallow depths, (*e.g.* neck or plug) but the presence of a large quantity of fluids suggests that intrusion occurred in wet permeable sediments. Fluids from secondary boiling of the magma, coupled with the generation of steam in the surrounding sediments, caused fracturing and brecciation of both the chilled margin of the intrusive body and surrounding sediment strata. The lack of significant thermal metamorphic effects suggests a small size intrusion occurred in a short time span Although infrequent this emplacement style has already been recognised in Taylor Glacier and in Allan Hills (Craw & Findlay, 1984; Grapes et al., 1973).

this area as being recorded in CRP-2 at 280 mbsf and dated at 24.22 Ka (McIntosh, 2001).

As in CRP-1, no clasts having compositional or petrographical characters attributable to the SPCT has been found. SPCT rocks cap the Jurassic lavas, and may represent a good marker in the reconstruction of the erosion history of the area. In contrast to CRP-1, clasts in CRP-3, that could have been derived from the Kirkpatrick Basalt, are very common. The increase in subalkaline basalt clasts mainly derived from Ferrar Supergroup rocks indicate that a large part of the erosion of the Jurassic units must have taken place in Eocene-Oligocene time (Cape Roberts Science Team, 2000).

Finally, though heavily affected by alteration, the intrusive body shows a clear subalkaline affinity, which rules out a Cainozoic age and indicates that it belongs to the Jurassic Ferrar Supergroup. This intrusive body can be considered as one of the many

REFERENCES

Allibone A.H. 1992. Low-Pressure High-Temperature Metamorphism of Koettlitz Group schists, Taylor Valley and Upper Ferrar Glacier Area, South Victoria Land, Antarctica. *New Zealand Journal of Geology and Geophysics*, 35, 115-127.

Allibone A.H, Cox S.C., Graham I.J., Smillie R.W., Johnstone R.D., Ellery S.G., & Palmer K., 1993. Granitoids of the Dry Valleys area Southern Victoria Land, Antarctica - Plutons, field, relationships, and isotopic dating. *New Zealand Journal of Geology and Geophysics*, 36, 281-297.

Armienti P., Messiga B. & Vannucci R., 1998. Sand provenance from Major and Trace element Analyses of Bulk rock and sand grains. *Terra Antartica*, 5, 589-599.

Armienti P., Pompilio M., & Tamponi M., 2001. Sand provenance from major and trace element analyses of bulk rock and sand grains from CRP-2/2A, Victoria Land Basin, Antarctica. This volume.

Bozzo E., Damaske D., Caneva G., Chiappini M., Ferraccioli F., Gambetta M. & Meloni A., 1997. A High Resolution Aeromagnetic Survey over Proposed Drill Sites Off Shore of Cape Roberts in the Southwestern Ross Sea (Antarctica). In: Ricci C.A. (ed.), *The Antarctic Region: Geological Evolution and Processes*. Terra Antartica Publication, Siena, 1129-1134.

Brotzu P., Capaldi G., Civetta L., Melluso L. & Orsi G., 1988. Jurassic Ferrar Dolerites and Kirkpatrick Basalt in northern Victoria Land (Antarctica): Stratigraphy, Geochronology, and Petrology. *Memorie della Società Geologica Italiana*, **13**, 97-116.

Cape Roberts Science Team, 2000. Studies form the Cape Roberts Project, Ross Sea, Antarctica. Initial Report on CRP-3. *Terra Antartica*, **7**, 1-209.

Craw D. & Findlay R. H., 1984. Hydrothermal alteration of Lower Ordovician granitoids and Devonian Beacon Sandstone at Taylor Glacier, McMurdo Sound, Antarctica. *New Zealand Journal of Geology and Geophysics*, **27**, 465-475.

Elliot D.H., 2000. Stratigrapby of Jurassic Pyroclastic rocks in the Transarctic Mountains. Journal of African Earth Sciences, **31**, 77-89.

Elliot D.H., 1996. The Hanson Formation: a new stratigraphic unit in Transantarctic Mountains, Antarctica. *Antarctic Science*, **8**, 389-394.

Elliot D.H., Fleming T.H., Haban M.A., & Siders M.A., 1995. Petrology and mineralogy of the Kirkpatrick basalt and Ferrar dolerite, Mesa range region, North Victoria Land, Antarctica. *Contributions to Antarctic Research IV - Antarctic research series*, **67**, 103-141.

Elliot D.H., Haban M.A., Siders M.A., 1986. The Exposure Hill Formation, Mesa Range. In Stump, E. (Ed.), Geological Investigations in Northern Victoria Land. American Geophysical Union, Washington DC, *Antarctic research series*, **46**, 267-284.

Fleming T.H., Elliot D.H., Jones L.M., Bowman J.R., & Siders M.A., 1992. Chemical and isotopic variations in an iron-rich lava flow from the Kirkpatrick Basalt, north Victoria Land, Antarctica: implications for low temperature alteration. *Contributions to Mineralogy and Petrology*, **111**, 440-457.

Fleming T.H., Foland K.A. & Elliot D.H., 1995. Isotopic and chemical constraints on the crustal evolution aud source signature of Ferrar magmas, north Victoria Land, Antarctica. *Contributions to Mineralogy and Petrology*, **121**, 217-236.

Fitzgerald P., 1999. Cretaceous - Cenozoic Tectonic Evolution of the Antarctic Plate. *Terra Antartica Reports*, **3**, 109-130.

Franzini M. & Leoni, L., 1972. A full matrix correction in X-ray fluorescence analysis of rock samples: *Atti della Società Toscana di Scienze Naturali*, **79**, 7-22.

Floyd P.A. & Whinchester J.A., 1978. Identification and discrimination of altered and methamorphosed volcanic rocks using immobile elements. *Chemical Geology*, **21**, 291-306.

Gamble J., Barrett P.J. & Adams C.J., 1986. Basaltic clasts from

Unit 8. In: Barrett P.J. (ed.), *Antarctic Cenozoic history, MSSTS-1 drillhole*, *DSIR Bulletin*, **237**.

Grapes R., Gamble J. & Palmer P., 1989. Basal dolerite boulders. In: Barrett P.J. (ed.), *Antarctic Cenozoic history from CIROS-1 drillhole, McMurdo Sound. DSIR Bulletin*, **245**, 169-174.

Grapes R.H., Reid D.L. & McPherson J. G., 1973. Shallow dolerite intrusion and phreatic eruption in the Allan Hills region. *New Zealand Journal of Geology and Geophysics*, **17**, 563-579.

Hornig I., 1993. High-Ti and Low-Ti tholeites in the Jurassic Ferrar Group, Antarctica. *Geologisches Jahrbuch*, **E47**, 335-369.

Kyle P.R., 1981. Mineralogy and geochemistry of a basanite to phonolite sequence at Hut Point Peninsula, Antarctica, based on core from Dry Valley Drilling Project Drillholes 1, 2 and 3. *Journal of Petrology*, **22**, 451-500.

Kyle P.R., 1998. Ferrar dolerite clasts from CRP-1 drillcore. *Terra Antartica*, **5**, 611-612.

Kyle P.R., 1990. McMurdo Volcanic Group-Western Ross Embayment. Introduction. In: *Volcanoes of the Antarctic Plate & Southern Oceans*. pp. 19-134. Antarctic Research Series, American Geophysical Union, Washington.

LeMasurier W.E., 1990. Late Cenozoic volcanism on the Antarctic Plate: an overview. In: *Volcanoes of the Antarctic Plate & Southern Oceans*. pp. 1-17. Antarctic Research Series, Washington.

Leoni L. & Saitta M., 1976. X-ray fluorescence analysis of 29 trace elements in rocks and mineral standards: *Rendiconti della Società Italiana di Mineralogia e Petrologia*, **32**, 497-510.

Leterrier J., Maury R.C., Thonon P., Girard D. & Marchal M., 1982. Clinopyroxene composition as a method of identification of the magmatic affinities of palaeo-volcanic series. *Earth Planetary Science Letters*, **59**, 139-154.

McIntosh W.C., 2001. $^{40}Ar/^{39}Ar$ Chronology of Tephra and Volcanic Clasts in CRP-2A, Ross Sea, Antarctica. *Terra Antartica*, **7**, 621-630.

Morimoto, N., 1988. Nomenclature of pyroxenes. *Mineralogy and Petrology*, **39**, 55-76.

Nesbitt H. W. & Young G. M., 1982. Early Proterozoic climates and plate motions inferred from major element chemistry of lutites. *Nature*, **299**, 715-717.

Nesbitt H. W. & Young G. M., 1989. Formation and diagenesis of a weathering profiles. *Journal of Geology*, **97**, 129-147.

Roland N. W. & Wörner G., 1996. Kirkpatrick flows and associated pyroclastics: new occurrences, definition, and aspects of a Jurassic Transantarctic rift. *Geologisches Jahrbuch*, **B89**, 97-121.